Evidence of Smaller 1/F Noise in AlScN-Based Oscillators Compared to AlN-Based Oscillators

A. Lozzi, M. Liffredo, E. Ting-Ta Yen, J. Segovia-Fernandez, L.G. Villanueva

The version of record of this article appeared in A. Lozzi, M. Liffredo, E. T. Yen, J. Segovia-Fernandez and L. G. Villanueva, "Evidence of Smaller 1/F Noise in AlScN-Based Oscillators Compared to AlN-Based Oscillators," in *Journal of Microelectromechanical Systems*, vol. 29, no. 3, pp. 306-312, June 2020 and can be found at https://doi.org/10.1109/JMEMS.2020.2988354

EVIDENCE OF SMALLER 1/F NOISE IN ALSCN-BASED OSCILLATORS COMPARED TO ALN-BASED OSCILLATORS

Andrea Lozzi[1*]*, Marco Liffredo*[1]*, Ernest Ting-Ta Yen*[2]*, Jeronimo Segovia-Fernandez*[2]*, and Luis Guillermo Villanueva*[1]

[1]Advanced NEMS Lab, École Polytechnique Fédérale de Lausanne (EPFL), Lausanne, SWITZERLAND
[2]Kilby Labs, Texas Instruments Inc., Santa Clara, USA

ABSTRACT

In this paper we investigate the direct effect of resonator quality factor (Q) on the oscillator phase noise. We use 2-port contour mode resonators (CMRs), fabricated both with aluminum nitride (AlN) and aluminum scandium nitride (AlScN), as the frequency-determining element in the oscillator circuit. Over 70 oscillator configurations are tested using resonators with different Q and with different piezoelectric layer. The testing of so many devices is possible because, in our setup, interfacing the circuit to the resonator is streamlined using RF probes. Our results show that higher resonator Q yields better frequency stability of the oscillator, for both AlN and AlScN CMRs. Interestingly, the comparison between AlN-based oscillators and AlScN-based oscillators with equal Q shows that AlScN-based oscillators' Phase Noise is up 10 dBc/Hz better than the AlN oscillator at 1 kHz offset frequency, suggesting different intrinsic resonator flicker noise of the two piezoelectric layers.

KEYWORDS

Oscillator, phase noise, aluminum nitride, aluminum scandium nitride, contour mode resonators,

INTRODUCTION

The internet-of-things (IoT) relies on the concept of hyper connectivity between many physical objects. In the near future, devices will exist in a connected network rather than in isolation, where data exchange will play a crucial role. Ideally, each node of the network will be equipped with a communication module. In this context, the RF front ends will need to meet new stringent requirements in terms of chip size, power consumption and cost [1].

Microelectromechanical systems (MEMS) are good candidates to promote high performance and yet more flexible radio architectures. Contour Mode Resonators (CMRs) [2] are an appealing class of piezoelectric MEMS resonators as their operating frequency can be largely tuned by design unlike Film Bulk Acoustic Resonators (FBARs) [3]. This unique feature can enable multi-frequency reconfiguration on the same chip and new RF radios architectures [4, 5]. Following FBAR commercialization, AlN has been the gold standard piezoelectric material to make RF filters. A broad range of AlN-based devices has been studied [38]. AlN CMRs have demonstrated Q values of up to 4000 [6-8], whereas the electromechanical coupling is limited to about 2% [9]. AlScN is gaining consensus in the community as the AlN alternative given the similar fabrication and its larger piezoelectric response, often obtained at the expenses of a reduced Q [10, 11], CMR resonators allow to define their resonance frequency via lithography and have been investigated in a broad range of materials including but not limited to AlN, such as GaN [40], PZT [41], ZnO [42]. In the new RF front-ends, MEMS-based elements for frequency generation and frequency control will be necessary. For this reason, filters and oscillators based on MEMS have been proposed since they foster monolithic integration to the circuitry in a small form factor. In this paper we focus on the demonstration of MEMS-based oscillators which, compared to oscillators based on SAW and quartz resonators [39], have not yet been able to offer on par noise performance, assessed via the phase noise (PN). PN is a direct measure of the oscillator frequency stability [12] and is defined as in Eq. 1 according to Leeson's model [13, 14]:

$$\mathcal{L}(f_m) = 10log\left[\frac{1}{2}\left(\left(\frac{f_0}{2Qf_m}\right)^2+1\right)\left(\frac{f_c}{f_m}+1\right)\left(\frac{Fk_BT}{P_s}\right)\right] \qquad (1)$$

where f_0 is the carrier output frequency, f_m is the offset frequency, f_c is the corner frequency, F is the noise factor of the amplifier, and P_s is the power at the input of the amplifier. PN improves when Q and P_s increase.

In order to enhance the noise performance of MEMS-based oscillators, improving the resonator Q has been proposed [15], as well as using nonlinear resonators [16, 17] or using parametric schemes [12, 16, 18, 19]. The latter approaches imply a more complex oscillator setup, whereas the former ideally permits to work directly on the design optimization of the resonator to improve the noise performance of the oscillator circuit.

AlN CMR-based oscillators have been demonstrated with PN value between -90 dBc/Hz and -100 dBc/Hz at 1 kHz offset frequency and around 200 MHz carrier frequency [20, 21]. Also, only recently, groups demonstrated that a crystal-less RF module is possible while maintaining good performance [22, 23]. Although some works have already tried to clarify the effect of Q on the resonator flicker noise [24-26] and to quantify frequency fluctuation of CMRs [27], direct measurements of phase noise as a function of the resonator Q for many resonators are still lacking, because of the typically laborious measurement setups (i.e. wirebonding of a single CMR).

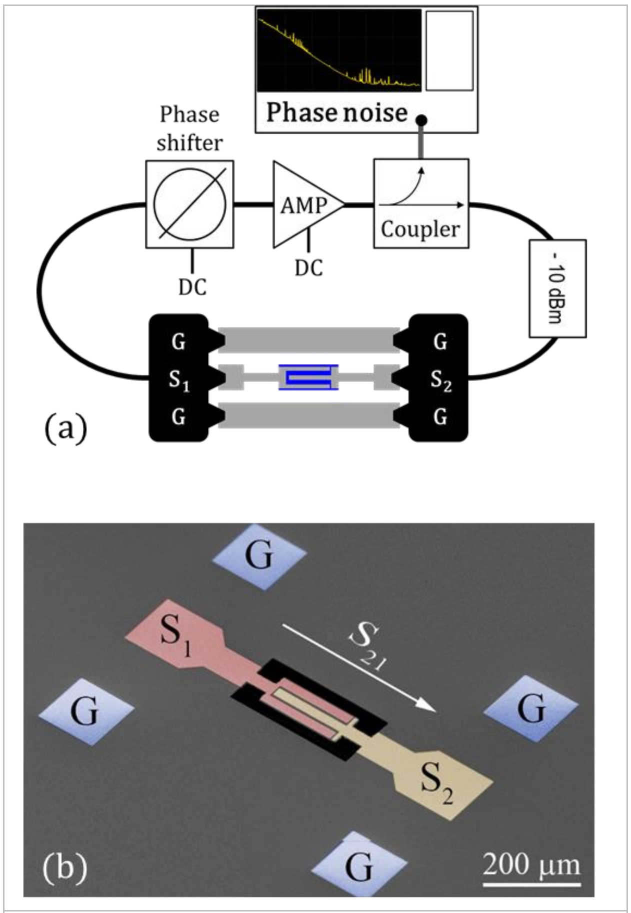

Figure 1: (a) Schematic of the phase noise measurement setup. The oscillator is composed of a phase shifter and an amplifier to meet the Barkhausen's stability criteria for oscillation. RF probes are used to contact the resonator and close the loop. An attenuator is placed in the loop to guarantee operation in the linear regime of the CMR (b) SEM picture of a fabricated 2-port AlScN CMR. The electrical probing configuration is reported. The input port pad is labeled as S_1 *(red) whereas the output port pad is labeled as* S_2 *(yellow). The common ground pads are in blue.*

In this paper we use 2-port CMRs made of either AlN or AlScN (17% Sc doping) as the frequency-determining element in the oscillator. We use off-the-shelf discrete components to build an oscillator circuit that is composed of an amplifier, a phase shifter and an attenuator (Fig. 1). The amplifier provides the gain to sustain the oscillation and it also saturates the oscillation because of its inherent nonlinearity. The phase shifter sets the phase-lag in the loop and consequently the carrier frequency within the range that is enabled by the amplifier gain and the resonator. The attenuator helps us control the power coming into the resonator to avoid it entering its nonlinear regime. The resonator acts as a passive frequency selective element. Importantly, we use RF probes to contact the resonator and close the oscillator loop. This, unlike wire bonding of the CMR to a PCB, allows fast testing of a large number of resonators with different properties, including different Q, enabling direct measurement of the oscillator PN trend as a function of the resonator Q.

METHODS

A 4-mask process flow is used to fabricate 2-port AlN and AlScN CMRs (Fig. 1b) (transducers). The stack is composed of 100 nm of Pt for the bottom metal plate, 1.2 µm for the AlScN and ALN layers and 100 nm of Pt for the top electrodes [28]. In a previous work, we reported Q as high as 1500 and electromechanical coupling up to 4.5% for 1 port AlScN CMRs [10].

We use a HP8719D network analyzer to record the transmission scattering parameter S_{21}. The electrical response is fitted to a mBVD model in order to extract the motional parameters, the resonator Q, and the resonator resonance frequency (f_r). In order to obtain a wide range of Q values, two geometrical design parameters are swept: the bus length (B) and the anchor width (W_a) (Fig. 2).

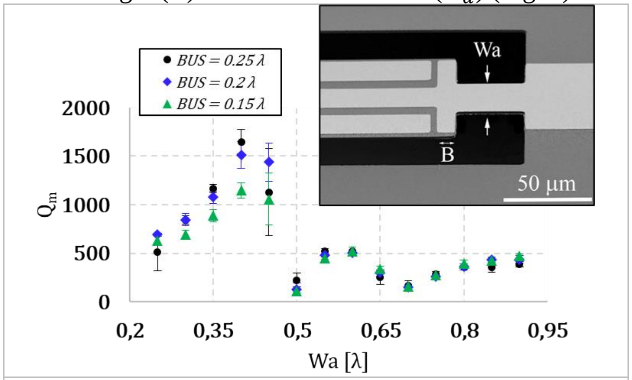

Figure 2: (a) Loaded Q as function of W_a *for resonators* 3.5λ *long and with fixed* $L_a = \lambda$. *Each point is the average response of 3 identical devices, and we also show the deviation in the values of the 3 devices. Within the plot, three configurations are shown:* $B = 0.15\lambda$ *(green triangles),* $B = 0.2\lambda$ *(blue diamonds), and* $B = 0.25\lambda$ *(black circles). In the three different configurations it is evident the presence of a peak in the region* $W_a = 0.45\lambda - 0.5\lambda$. *In the inset, an SEM picture of a fabricated CMR is shown, with the two geometrical parameters swept in this study: B and* W_a.

From Fig. 2 we see that B does not contribute much to Q variation, whereas W_a has a lot of influence [6]. For this reason, when W_a is varied in the range between 0.25λ and 0.9λ, the measured (loaded) Q spans from about 150 to 1600 for AlScN and from about 600 to 2000 (Fig. 2) for AlN. For AlScN resonators, C_0 goes from 231 fF to 311 fF, Rm goes from 71Ω to 536Ω, and resonance frequency goes from 191.71 to 194.14 MHz. Since the resonators are 2-ports, we calculate the piezoelectric coupling coefficient k_t^2 by using $k_t^2 = \frac{\pi^2}{8}\frac{C_m}{C_0}$, and it goes from 2.17% to 3.12%. After extracting the resonator parameters, an amplifier (*AU-1442, L3 Narda-Miteq*) and a phase shifter (*SO-06-411, Pulsar*) are used to create an oscillator, similarly to what previously described in [17]. A modification to this setup is made: instead of wire bonding the device to a PCB in order to interface the resonator to the remaining electronics, RF probes are used to directly contact the resonator (Fig. 1a). This streamlines the connection of many different resonators to the oscillator circuit, ultimately allowing fast assessment of many oscillators' PN performance. In this study, this flexibility allows a proper quantitative assessment of the PN trend when the resonator Q varies. In the oscillator setup, the addition of a 10 dB attenuator in the close loop guarantees that the resonator operates at -10 dBm input power, i.e. in its linear regime. The amplifier and phase shifter are used to meet the Barkhausen's stability criteria for oscillation. For each oscillator, PN is measured using an E5052A Signal Source Analyzer. Using GSG probes allows also to quickly compare AlScN and AlN resonators: if Q is the same, keeping the same layout and the same oscillator loop, any difference in PN mainly comes from the different material employed.

MEASUREMENT TECHNIQUE

We start by characterizing the resonators in open loop by connecting the GSG probes to both ports and directly to a Vector Network Analyzer (HP8719D). In Fig. 3 we can see the admittance response (Y_{21}) of the resonators with the maximum and minimum Q and R_m.

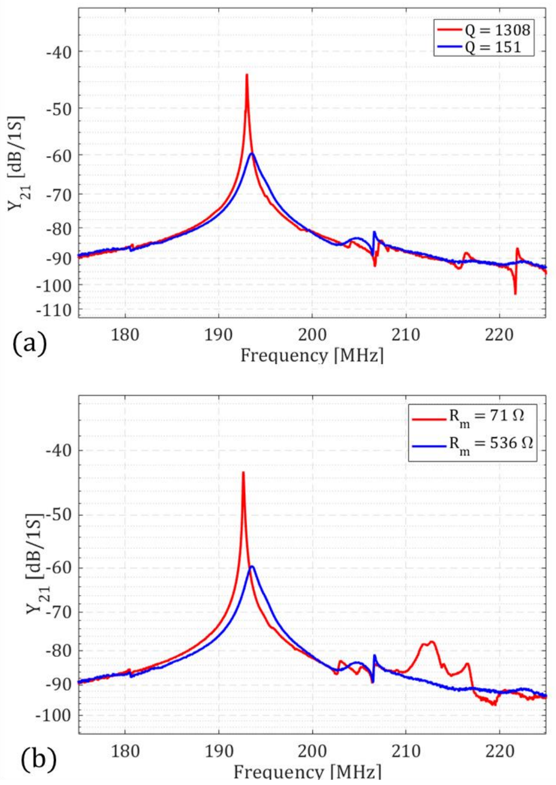

Figure 3: Admittance plots comparing maximum and minimum R_m AlScN resonators (a) and maximum and minimum Q (b)

As seen in Eq. 1, PN is inversely proportional to Q and to the carrier power. Thus, a fair comparison between diverse resonators implies maintaining the same carrier power level. For this reason, the carrier power in the close loop is kept to -10 dBm across all the resonators (via amplifier). This means that the power supplied to the amplifier in the loop is different depending on R_m. Indeed, for the maximum and minimum values of R_m, we find a power consumption in the amplifier of 83mW and 121mW respectively. However, it is possible to lock the oscillator at different operational points of the resonator, depending on the phase shift in the loop.

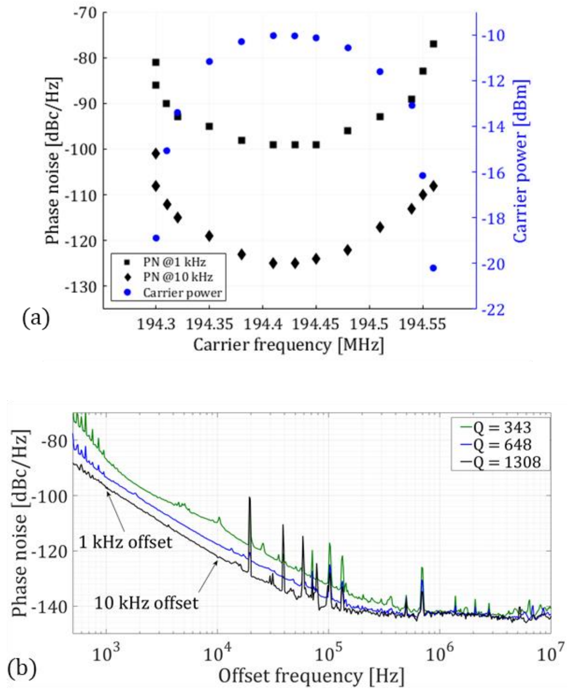

Figure 4: (a) Phase noise at 1 kHz (black squares) and 10 kHz (black diamonds) offset frequency; as a function of the oscillation carrier frequency, tuned via the phase shifter. In blue dots, the carrier power in the loop is shown. In this case we keep constant the amplifier power supply. (b) Example of phase noise as a function of the offset frequency for three different resonator quality factors: $Q = 343$ (green line), $Q = 648$ (blue line), and $Q = 1308$ (black line). Increasing the resonator Q results in an improvement of PN.

We study the noise levels when varying the phase shift induced by the phase shifter in the loop, and we observe that the carrier frequency changes around the resonance peak of the resonator and that the PN can change up to 20 dB (Fig. 4a). The minimum value of PN is found when the oscillator operates exactly at the resonance frequency of the resonator. This is caused by two phenomena: (i) an increase in the insertion loss and (ii) a decrease of the phase vs. frequency slope of the resonator; both happening when we move away from the resonance frequency. Thus, before recording PN, we sweep around the resonance peak by tuning the phase shift in the loop and we ensure that we work at the same carrier power. PN is then measured. An example of this effect can be seen in Fig. 4a where the PN at 1 kHz and 10 kHz offset frequencies are shown vs the carrier frequency. Since the insertion loss across the resonator is minimum when operating on resonance; and the slope of the phase vs frequency response of the resonator is maximum when operating on resonance, we obtain the smaller PN at that point. We consider that operating the resonators on resonance and at the same carrier power level is crucial to compare between different resonators.

EXPERIMENTAL RESULTS

We extract PN from 100 Hz to 10 MHz offset frequencies focusing on the influence of the resonator Q on the oscillator PN. According to Eq. 1, an increase in the resonator Q is accompanied by a reduction in PN. Here we investigate if the Leeson's model successfully describes the behavior of MEMS-based oscillators.

Fig. 4b shows an example of PN as a function of the offset frequency for three different resonators, extracted following the measurement technique previously described. Clearly, different resonators' Q lead to different PN levels, with higher Q resonators offering enhanced PN performance. In particular, for $Q = 1308$, the measured PN is -98 dBc/Hz and -124 dBc/Hz at 1 kHz and 10 kHz offset frequencies, respectively. This correspond to a 5 and 11 dBc/Hz improvement at 1 kHz offset frequency with respect to $Q = 648$ and $Q = 343$, respectively. Similarly, at 10 kHz offset frequency the improvement is 6 and 14 dB. These results agree well with what is predicted by the Leeson's model: a factor of $2\times$ improvement in the resonator Q leads to a 6 dB decrease in PN. Moreover, the average slope of the three measurements at 10 kHz offset frequency goes as ~-20 dB/decade, as predicted by Eq. 1.

To investigate this relation and its dependence on the material further, we extract PN at 1 kHz offset frequency and the PN at 10 kHz offset frequency over 77 oscillators based on different AlN (13) and AlScN (64) devices. These two PN values are commonly used as markers of the overall noise performance. The AlScN CMRs operate around 193 MHz, while the AlN CMRs operate at around 234 MHz. The Q values span from about 150 to 1600 for the AlScN CMRs, while from about 600 to 2000 for the AlN CMRs. The overlap of Q values between AlN and AlScN allows direct study of the influence of the material in the noise performance.

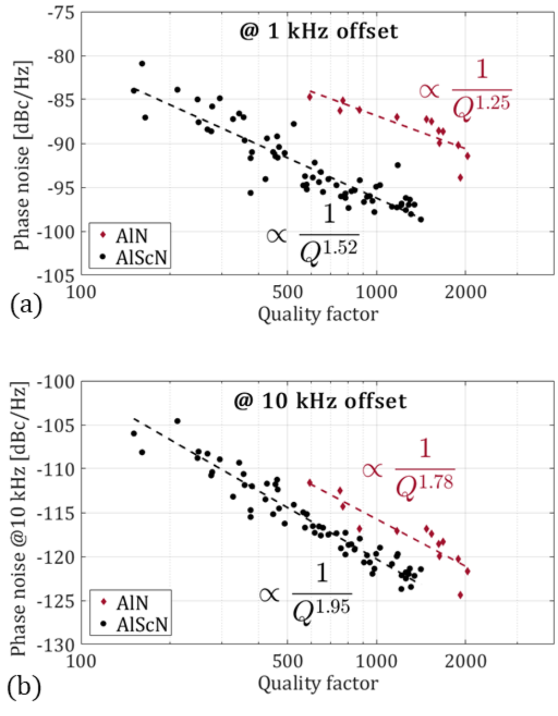

Figure 5: (a) Measured phase noise as a function of the resonator quality factor at 1 kHz (a) and 10 kHz (b) offset frequency: 64 AlScN-based oscillators (black dots) and 13 AlN-based oscillators (red diamonds) are measured. The black and red dashed line shows the fit to a power law function, which is reported in the inset for the AlN (red) and the AlScN (black) based oscillators.

In Fig. 5 the PN at 1 kHz offset frequency and at 10 kHz offset frequency as a function of the resonator Q is reported for AlN and AlScN-based oscillators. The AlN PN is scaled by 41 MHz to account for the slightly higher carrier frequency compared to AlScN. The data points are fitted to a power law function to extract the PN trend. At 1 kHz offset frequency the AlN oscillator noise scales as $Q^{-1.25}$ while the AlScN oscillator scales as $Q^{-1.52}$. In contrast, at 10 kHz offset frequency the AlN oscillator noise scales as $Q^{-1.78}$ and the AlScN oscillator scales as $Q^{-1.95}$. The latter is close to the theoretical Q^{-2} predicted by Leeson. As a matter of fact, as it is exemplary shown in Fig. 4b, at 10 kHz offset frequency the noise slope is -20 dB/decade for the AlScN oscillators, confirming Leesons' theory. In all the other cases, the dependence of PN on Q deviates from the theoretical value and we confirm that the slope also does deviate from the prediction.

Importantly, from the results it is seen that the AlScN and AlN oscillators performance do not lay on the same trend line. If only Q is considered as a defining parameter of the noise level, it should not matter the piezoelectric layer used in the electroacoustic transduction. In Fig. 6 we show a comparison of one AlN-based oscillator and an AlScN-based oscillator, both having the same $Q = 1450$. Since not only Q, but everything in the system is almost identical (amplifier, phase shifter, carrier power, etc.), the only possible conclusion is that the difference is caused due to the resonator material. Interestingly, the two PN profiles are different. The AlN shows a 10 dB and a 5 dB worse PN than AlScN at 1 kHz and 10 kHz offset frequencies, respectively. Moreover, the slope of the two PN profiles at 10 kHz offset frequencies is about -20 dB/decade for AlScN and about -30 dB/decade for AlN. Other works reported similar slope than us for AlN-based oscillators [17, 19, 20]. In the case of AlScN, to our knowledge we are the first group ever reporting PN. Our conclusion from the presented data is that an additional noise source to those considered in Leeson's model. We believe this to be intrinsic fluctuations of the resonance frequency of the resonators [29], which directly feed into the phase noise of the oscillator, are in most cases $1/f$ in nature (which translates to slopes of -30 dB/decade in the PN plot). What our data shows is that the level of said fluctuations is different, and much smaller, in the case of AlScN as compared to AlN. We are currently developing an experimental setup to confirm or disprove this hypothesis, in order to directly measure the frequency jitter of each resonator, like indicated in the literature [25] [36][44].

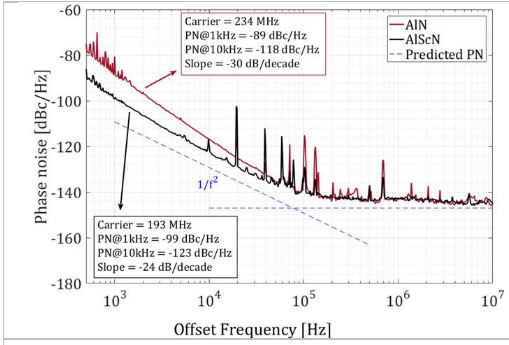

Figure 6: (a) Measured PN for an AlN-based oscillator with $Q = 1477$ (red) and for an AlScN-based oscillator with $Q = 1413$ (black). A predicted phase noise is also derived analytically (blue dashed line).

Tech	Paper	Freq. (MHz)	PN 1 kHz (dBc/Hz)	PN 10 kHz (dBc/Hz)	PN 1 MHz (dBc/Hz)	FoM 1 kHz	FoM 10 kHz	FoM 1 MHz	P supply (mW)
AlScN CMR (this work)		*193*	*-99*	*-123*	*-142*	*-185,52*	*-189,52*	*-168,52*	*83*
AlN CMR (this work)		*234*	*-91*	*-120*	*-142*	*-178,94*	*-187,94*	*-169,94*	*88*
AlN CMR	*[35]*	*1050*	*-91*	*-106*	*-145*	*-205,98*	*-209,98*	*-199,98*	*3.5*
AlN CMR	*[30]*	*222*	*-98*	*-130*	*-160*	*-194,93*	*-206,93*	*-196,93*	*10*
AlN FBAR	*[43]*	*2000*	*-75*	*-100*	*-138*	*-217,04*	*-222,04*	*-220,04*	*0.025*
AlN-on-Si	*[33]*	*256*	*-82*	*-105*	*-145*	*-183,47*	*-186,47*	*-186,47*	*13*
AlN-on-SiO2	*[34]*	*4.9*	*-138*	*-154*	*-155*	*-221,01*	*-217,01*	*-178,01*	*0.12*
LiNbO3 IDT	*[31]*	*150*	*-84.4*	*-113*	*-146*	*-180,93*	*-189,53*	*-182,53*	*5*
LiNbO3 SAW	*[32]*	*503*	*NA*	*-122*	*-160*	*NA*	*NA*	*NA*	*NA*

Table 1: Comparison of phase noise from this work and from a selection of existing literature

$$FOM(f_m)=10\,log\big(\mathcal{L}(f_m)\big)+20\,log\left(\frac{f_m}{f_0}\right)+\ P_{DC}(dBm)$$

CONCLUSIONS

This paper presents a study on MEMS-based oscillators PN as function of the resonator Q. We do this measuring over 70 oscillator configurations using resonators with different Q. We fabricate 2-port CMRs resonators, both in AlN and AlScN (17% Sc content) with identical designs. In order to obtain a large pool of Q values, we design resonators with different anchor width dimensions. This is an effective way to tune the amount of anchor loss and ultimately the resonator Q: Q values from 150 to 2000 are obtained.

We select 64 AlScN CMRs operating at 193 MHz and 13 AlN CMRs operating at 234 MHz and we extract their Q and their resonant frequency via an electrical characterization. Afterwards, we use each of these resonators to build oscillators and measure the oscillator phase noise. This is possible because of a flexible oscillator setup: instead of wire bonding each single device to a PCB, the resonator is directly contacted via RF probes, allowing streamlined measurements across several resonators.

Moreover, in order to have a fair comparison across different resonators, we develop a measurement technique that builds on two conditions: (i) the carrier level is kept constant across all measurements (ii) the carrier frequency is finely tuned via the phase shifter to minimize phase noise, i.e. matching the resonator resonance frequency. We show that it is crucial to meet both conditions to compare phase noise obtained from different resonators.

Our results show that Q indeed plays a role in defining the oscillator noise performance: higher Q reduce the noise level at the small offset frequencies. We fit the PN at 1 kHz and 10 kHz offset frequencies to a power law, and show that PN follows Leesons' theory: when the PN slope is -20 dB/decade, then the phase noise decreases as Q^{-2}. In other words, a factor 2 × improvement in Q results in 6 dB noise reduction. More interestingly, our results show that AlScN-based oscillators perform up to 10 dB at 1 kHz offset frequency better than AlN-based oscillators with the same resonator Q. While studies are ongoing to fully understand the cause of this difference, we believe that this finding can further promote the use of AlScN in industrial settings. Moreover, our measurement technique can help streamline the assessment of PN at a testing level and foster a deeper understanding of the noise roots in MEMS-based oscillators.

ACKNOWLEDGEMENTS

The authors would like to acknowledge Dr. David Ruffieux for the fruitful discussion on phase noise and the Center for Micronanotechnology (CMi) for their support in the resonators fabrication. This work was funded by Grant No. PP00P2_170590 of the Swiss SNF and by the CMRs Radios project from Texas Instruments.

REFERENCES

[1] R. Thirunarayanan, A. Heragu, D. Ruffieux, and C. Enz, "Complementary BAW oscillator for ultra-low power consumption and low phase noise," Analog Integrated Circuits and Signal Processing, vol. 73, pp. 769-777, 2012.

[2] G. Piazza, P. J. Stephanou, and A. P. Pisano, "Piezoelectric aluminum nitride vibrating contour-mode MEMS resonators," Journal of Microelectromechanical systems, vol. 15, pp. 1406-1418, 2006.

[3] R. C. Ruby, P. Bradley, Y. Oshmyansky, A. Chien, and J. Larson, "Thin film bulk wave acoustic resonators (FBAR) for wireless applications," in 2001 IEEE Ultrasonics Symposium. Proceedings. An International Symposium (Cat. No. 01CH37263), 2001, pp. 813-821.

[4] G. Piazza, "Integrated aluminum nitride piezoelectric microelectromechanical system for radio front ends," Journal of Vacuum Science & Technology A: Vacuum, Surfaces, and Films, vol. 27, pp. 776-784, 2009.

[5] C. T.-C. Nguyen, "MEMS technology for timing and frequency control," IEEE transactions on ultrasonics, ferroelectrics, and frequency control, vol. 54, pp. 251-270, 2007.

[6] J. Segovia-Fernandez, M. Cremonesi, C. Cassella, A. Frangi, and G. Piazza, "Anchor losses in AlN contour mode resonators," Journal of microelectromechanical systems, vol. 24, pp. 265-275, 2014.

[7] C. Cassella, N. Singh, B. W. Soon, and G. Piazza, "Quality factor dependence on the inactive regions in AlN contour-mode resonators," Journal of Microelectromechanical Systems, vol. 24, pp. 1575-1582, 2015.

[8] A. Lozzi, A. De Pastina, E. T.-T. Yen, and L. G.

Villanueva, "Engineered acoustic mismatch for anchor loss control in contour mode resonators," Applied Physics Letters, vol. 114, p. 103502, 2019.

[9] P. Muralt, "Piezoelectric thin films for MEMS," Integrated Ferroelectrics, vol. 17, pp. 297-307, 1997.

[10] A. Lozzi, E. T.-T. Yen, P. Muralt, and L. G. Villanueva, "Al 0.83 Sc 0.17 N Contour-Mode Resonators With Electromechanical Coupling in Excess of 4.5%," IEEE transactions on ultrasonics, ferroelectrics, and frequency control, vol. 66, pp. 146-153, 2018.

[11] L. Colombo, A. Kochhar, C. Xu, G. Piazza, S. Mishin, and Y. Oshmyansky, "Investigation of 20% scandium-doped aluminum nitride films for MEMS laterally vibrating resonators," in 2017 IEEE International Ultrasonics Symposium (IUS), 2017, pp. 1-4.

[12] C. Cassella, S. Strachan, S. W. Shaw, and G. Piazza, "Phase noise suppression through parametric filtering," Applied Physics Letters, vol. 110, p. 063503, 2017.

[13] D. Lesson, "A simple model of feedback oscillator noise spectrum," proc. IEEE, vol. 54, pp. 329-330, 1966.

[14] E. Rubiola, "The Leeson effect-Phase noise in quasilinear oscillators," arXiv preprint physics/0502143, 2005.

[15] T. H. Lee and A. Hajimiri, "Oscillator phase noise: A tutorial," IEEE journal of solid-state circuits, vol. 35, pp. 326-336, 2000.

[16] L. Villanueva, E. Kenig, R. Karabalin, M. Matheny, R. Lifshitz, M. Cross, et al., "Surpassing fundamental limits of oscillators using nonlinear resonators," Physical review letters, vol. 110, p. 177208, 2013.

[17] J. Segovia-Fernandez, C. Cassella, and G. Piazza, "Close-in phase noise reduction in an oscillator based on 222 MHz non-linear contour mode AlN resonators," in 2013 Joint European Frequency and Time Forum & International Frequency Control Symposium (EFTF/IFC), 2013, pp. 13-16.

[18] L. G. Villanueva, R. B. Karabalin, M. H. Matheny, E. Kenig, M. C. Cross, and M. L. Roukes, "A nanoscale parametric feedback oscillator," Nano letters, vol. 11, pp. 5054-5059, 2011.

[19] C. Cassella and G. Piazza, "Low phase-noise autonomous parametric oscillator based on a 226.7 MHz AlN contour-mode resonator," IEEE transactions on ultrasonics, ferroelectrics, and frequency control, vol. 62, pp. 617-624, 2015.

[20] G. Piazza, A. Tazzoli, N. Miller, J. Segovia, C. Cassella, J. Koo, et al., "Dynamics of microscale thin film AlN piezoelectric resonators enables low phase noise UHF frequency sources," in 2013 Joint European Frequency and Time Forum & International Frequency Control Symposium (EFTF/IFC), 2013, pp. 555-558.

[21] M. Rinaldi, C. Zuo, J. Van der Spiegel, and G. Piazza, "Reconfigurable CMOS oscillator based on multifrequency AlN contour-mode MEMS resonators," IEEE Transactions on Electron Devices, vol. 58, pp. 1281-1286, 2011.

[22] D. Griffith, E. T.-T. Yen, K. Tsai, T. Kallerud, and B. Goodlin, "A crystal-less bluetooth low energy radio using a MEMS-based frequency reference system," in 2017 Joint Conference of the European Frequency and Time Forum and IEEE International Frequency Control Symposium (EFTF/IFCS), 2017, pp. 181-184.

[23] S. Zaliasl, J. C. Salvia, G. C. Hill, L. W. Chen, K. Joo, R. Palwai, et al., "A 3 ppm 1.5× 0.8 mm 2 1.0 µA 32.768 kHz MEMS-Based Oscillator," IEEE Journal of Solid-State Circuits, vol. 50, pp. 291-302, 2014.

[24] E. Vaillant, F. Sthal, J. Imbaud, V. Soumann, P. Abbé, L. Arapan, et al., "Phase noise measurements of AlN contour-mode resonators with carrier suppression technique," IEEE transactions on ultrasonics, ferroelectrics, and frequency control, vol. 65, pp. 1943-1950, 2018.

[25] H. J. Kim, S. I. Jung, J. Segovia-Fernandez, and G. Piazza, "A study on flicker frequency noise of piezoelectric aluminum nitride resonators as a function of electrode design," in 2018 IEEE Micro Electro Mechanical Systems (MEMS), 2018, pp. 767-770.

[26] H. J. Kim, J. Segovia-Fernandez, and G. Piazza, "The impact of damping on flicker frequency noise of AlN piezoelectric MEMS resonators," Journal of Microelectromechanical Systems, vol. 26, pp. 317-324, 2017.

[27] N. Miller and G. Piazza, "Measurements of frequency fluctuations in aluminum nitride contour-mode resonators," IEEE transactions on ultrasonics, ferroelectrics, and frequency control, vol. 61, pp. 913-919, 2014.

[28] A. Lozzi, M. Liffredo, E. T.-T. Yen, J. Segovia-Fernandez, and L. G. Villanueva, "Phase Noise Measurements of Aluminum Scandium Nitride Oscillators," in 2019 20th International Conference on Solid-State Sensors, Actuators and Microsystems & Eurosensors XXXIII (TRANSDUCERS & EUROSENSORS XXXIII), 2019, pp. 909-912.

[29] M. Sansa, E. Sage, E. C. Bullard, M. Gély, T. Alava, E. Colinet, et al., "Frequency fluctuations in silicon nanoresonators," Nature nanotechnology, vol. 11, p. 552, 2016.

[30] C. Zuo, N. Sinha, J. Van der Spiegel, and G. Piazza, “Multifrequency Pierce Oscillators Based on Piezoelectric AlN Contour-Mode MEMS Technology,” Journal of Microelectromechanical Systems, vol. 19, no. 3, pp. 570–580, Jun. 2010.

[31] A. Kourani et al., “A 150 MHz voltage controlled oscillator using lithium niobate RF-MEMS resonator,” in 2017 IEEE MTT-S International Microwave Symposium (IMS), 2017, pp. 1307–1310.

[32] S. Tanaka, K. Park, and M. Esashi, “Lithium-niobate-based surface acoustic wave oscillator directly integrated with CMOS sustaining

amplifier," IEEE Transactions on Ultrasonics, Ferroelectrics, and Frequency Control, vol. 59, no. 8, pp. 1800–1805, Aug. 2012.

[33] H. M. Lavasani, W. Pan, and F. Ayazi, "An electronically temperature-compensated 427MHz low phase-noise AlN-on-Si micromechanical reference oscillator," in 2010 IEEE Radio Frequency Integrated Circuits Symposium, 2010, pp. 329–332.

[34] Z. Z. Wu, V. A. Thakar, A. Peczalski, and M. Rais-Zadeh, "A low phase-noise Pierce oscillator using a piezoelectric-on-silica micromechanical resonator," in 2013 Transducers Eurosensors XXVII: The 17th International Conference on Solid-State Sensors, Actuators and Microsystems (TRANSDUCERS EUROSENSORS XXVII), 2013, pp. 490–493.

[35] C. Zuo, J. V. Der Spiegel, and G. Piazza, "1.05-GHz CMOS oscillator based on lateral- field-excited piezoelectric AlN contour- mode MEMS resonators," IEEE Transactions on Ultrasonics, Ferroelectrics, and Frequency Control, vol. 57, no. 1, pp. 82–87, Jan. 2010.

[36] E. Vaillant et al., "Phase Noise Measurements of AlN Contour-Mode Resonators With Carrier Suppression Technique," IEEE Transactions on Ultrasonics, Ferroelectrics, and Frequency Control, vol. 65, no. 10, pp. 1943–1950, Oct. 2018.

[37] High-Frequency Oscillator Design for Integrated Transceivers, vol. 748. Boston: Kluwer Academic Publishers, 2005.

[38] C. Cassella, Y. Hui, Z. Qian, G. Hummel, and M. Rinaldi, "Aluminum Nitride Cross-Sectional Lamé Mode Resonators," Journal of Microelectromechanical Systems, vol. 25, no. 2, pp. 275–285, Apr. 2016.

[39] C. S. Lam, "A review of the recent development of MEMS and crystal oscillators and their impacts on the frequency control products industry," in 2008 IEEE Ultrasonics Symposium, 2008, pp. 694–704.

[40] A. Ansari, V. J. Gokhale, J. Roberts, and M. Rais-Zadeh, "Monolithic integration of GaN-based micromechanical resonators and HEMTs for timing applications," in 2012 International Electron Devices Meeting, 2012, pp. 15.5.1-15.5.4.

[41] S. S. Bedair et al., "Low loss micromachined lead zirconate titanate, contour mode resonator with 50Ω termination," in 2012 IEEE 25th International Conference on Micro Electro Mechanical Systems (MEMS), 2012, pp. 708–712.

[42] G. K. Ho, R. Abdolvand, and F. Ayazi, "High-order composite bulk acoustic resonators," in 2007 IEEE 20th International Conference on Micro Electro Mechanical Systems (MEMS), 2007, pp. 791–794.

[43] A. Nelson, J. Hu, J. Kaitila, R. Ruby, and B. Otis, "A 22µW, 2.0GHz FBAR oscillator," in 2011 IEEE Radio Frequency Integrated Circuits Symposium, 2011, pp. 1–4.

[44] P. Durdaut et al., "Noise Analysis and Comparison of Phase- and Frequency-Detecting Readout Systems: Application to SAW Delay Line Magnetic Field Sensor," IEEE Sensors Journal, vol. 19, no. 18, pp. 8000–8008, Sep. 2019, doi: 10.1109/JSEN.2019.2914965.

AUTHORS

Andrea Lozzi received his B.S.E. and M.Sc. degrees from Sapienza University (Rome, Italy) in 2010 and 2013, respectively. From 2013 to 2015, he was a research fellow at the Food and Drug Administration (Washington DC, USA) in the Center for Devices and Radiological Health. In 2015, he joined the Advanced NEMS Lab at the École Polytechnique Fédérale de Lausanne, (Switzerland), where he is currently pursuing the Ph.D. in Microsystems and Microelectronics. His research focuses on piezoelectric micro and nanoelectromechanical systems (M/NEMS) for RF wireless communication systems, with a particular interest in the design and characterization of micro electroacoustic resonators and their system integration. Andrea has authored and co-authored various publications in the fields of biomedical optics and MEMS.

Marco Liffredo received his B.Sc. in Physical engineering from Politecnico di Torino (Italy) in 2017 and his M.Sc. in Micro and Nanotechnologies for Integrated Systems form Politecnico di Torino (Italy), Intitut National Polytechnique de Grenoble (France) and EPFL (Switzerland) in 2019. After a brief collaboration with the Swatch Group he joined Advanced NEMS Laboratory in 2019 to work on piezoelectric MEMS Resonators. His research interests are RF Oscillators, IoT applications, and microfabrication techniques for thin film deposition.

Ernest Ting-Ta Yen (S'10-M'12) joined Kilby Labs in Texas Instruments (Santa Clara) as a MEMS technologist after receiving his Ph.D. degree in Mechanical Engineering from University of California, Berkeley in 2012; he also holds an M.S. degree in Electrical Engineering from UC Berkeley (2012) and a double B.S. degree in Electrical Engineering and Power Mechanical Engineering from National Tsing Hua University in Taiwan (2004). Dr. Yen's main research is focused on piezoelectric MEMS in RF applications. He developed the DBAR (dual-Bragg acoustic resonator) technology in TI, integrated and commercialized this technology into several system chips. He also leads university research projects in Kilby Labs focusing on RF MEMS, nano-mechanical circuit, and advanced packaging. Dr. Yen is an active reviewer of top MEMS journals including J-MEMS, Sensors etc. and was elected as the Vice-Chair of the IEEE SFBA (San Francisco Bay Area) MEMS & Sensor Chapter for 2016-2017.

Jeronimo Segovia-Fernandez (S'10-M'15) received his B.S. and M.S. degrees in Industrial Engineering with a specialization in Electrical and Electronics Engineering from the Universidad de Castilla-La Mancha (Spain) and the University of Birmingham (England) in 2008; and his Ph.D. degree in Electrical and Computer Engineering from Carnegie Mellon University in Pittsburgh (USA) in 2015. He was a postdoctoral researcher at the University of California, Davis, and worked as an R&D Hardware Engineer at Broadcom Limited. In 2018, he joined Texas Instruments Kilby Labs as an R&D Systems Engineer.

Dr. Segovia-Fernandez' main research has focused on piezoelectric Nano and MicroElectroMechanical Systems (N/MEMS) for sensing and Radio Frequency (RF) applications. His areas of interests include nano and microfabrication techniques, characterization and design of piezoelectric MEMS resonators, nonlinear dynamics, damping and phase noise analysis, analog and RF integrated circuit (IC) design, and MEMS-IC integration.

Guillermo Villanueva is a Tenure Track Assistant Professor at EPFL in Lausanne since 2016. He obtained his Ms. Sc. in Physics in 2002 from the University of Zaragoza (Spain) and his Ph.D. in Microelectronic Engineering from the Autonomous University of Barcelona in 2006 for his work on NEMS/MEMS for biodetection and scanning probes. He then worked as a post-doctoral researcher at EPFL, Caltech and DTU in the fields of nanofabrication, coupled and non-linear phenomena and dissipation in NEMS respectively. In 2013 he joined EPFL as a SNSF Assistant Professor to continue his research in fundamentals of nanomechanical systems for sensing and communications. In 2005 he was awarded the MNE Young Investigator Award for his PhD work, in 2008 he was awarded a Marie Curie Fellowship and in 2014 he was awarded the MEE Young Investigator Award.